

# **AEROELASTIC AIRWORTHINESS ASSESSMENT OF THE ADAPTIVE COMPLIANT TRAILING EDGE FLAPS**

Claudia Y. Herrera, Aerospace Engineer, and Natalie D. Spivey, Aerospace Engineer  
NASA Armstrong Flight Research Center, Edwards Air Force Base, California 93523

Shun-fat Lung, Structures Engineer  
Jacobs Engineering, NASA Armstrong Flight Research Center,  
Edwards Air Force Base, California 93523

Gregory Ervin  
FlexSys Inc., Ann Arbor, Michigan 48105

Peter Flick  
Air Force Research Laboratory, Air Vehicles Directorate,  
Wright-Patterson Air Force Base, Ohio, 45433

## **1. ABSTRACT**

**The Adaptive Compliant Trailing Edge (ACTE) demonstrator is a joint task under the National Aeronautics and Space Administration Environmentally Responsible Aviation Project in partnership with the Air Force Research Laboratory and FlexSys, Inc. (Ann Arbor, Michigan). The project goal is to develop advanced technologies that enable environmentally friendly aircraft, such as adaptive compliant technologies. The ACTE demonstrator flight-test program encompassed replacing the Fowler flaps on the Subsonic Aircraft Testbed, a modified Gulfstream III (Gulfstream Aerospace, Savannah, Georgia) aircraft, with control surfaces developed by FlexSys. The control surfaces developed by FlexSys are a pair of uniquely-designed unconventional flaps to be used as lifting surfaces during flight-testing to validate their structural effectiveness. The unconventional flaps required a multidisciplinary airworthiness assessment to prove they could withstand the prescribed flight envelope. Several challenges were posed due to the large deflections experienced by the structure, requiring non-linear analysis methods. The aeroelastic assessment necessitated both conventional and extensive testing and analysis methods. A series of ground vibration tests (GVTs) were conducted to provide modal characteristics to validate and update finite element models (FEMs) used for the flutter analyses for a subset of the various flight configurations. Numerous FEMs were developed using data from FlexSys and the ground tests. The flap FEMs were then attached to the aircraft model to generate a combined FEM that could be analyzed for aeroelastic instabilities. The aeroelastic analysis results showed the combined system of aircraft and flaps were predicted to have the required flutter margin to successfully demonstrate the adaptive compliant technology. This paper documents the details of the aeroelastic airworthiness assessment described, including the ground testing and analyses, and subsequent flight-testing performed on the unconventional ACTE flaps.**

## 2. NOMENCLATURE

1B	=	first bending
2B	=	second bending
3B	=	third bending
1T	=	first torsion
2T	=	second torsion
Accels	=	accelerometers
ACTE	=	Adaptive Compliant Trailing Edge
AFRC	=	Armstrong Flight Research Center
AFRL	=	Air Force Research Laboratory
FEM	=	finite element model
GIII	=	Gulfstream III aircraft
GVT	=	ground vibration test
ITS	=	inboard transition section
KCAS	=	knots calibrated airspeed
KEAS	=	knots estimated airspeed
MCC	=	Mission Control Center
NASA	=	National Aeronautics and Space Administration
OML	=	outer mold line
OTS	=	outboard transition section
P3.2B	=	Prototype 3.2B
SCRAT	=	Subsonic Research Aircraft Testbed

## 3. INTRODUCTION

Through the Small Business Innovation Research (SBIR) program, the Air Force Research Laboratory (AFRL) began supporting the development of adaptive compliant wing technology in 1998 with FlexSys, Inc. (Ann Arbor, Michigan) using various wing leading and trailing edge designs.<sup>1-5</sup> Numerous studies and flight-test demonstrations since have shown the aerodynamic benefits of an adaptive airfoil;<sup>6</sup> however, a full-scale flight demonstration was needed to establish confidence in and demonstrate the airworthiness of an adaptive, compliant structure with a continuous mold line.<sup>7-9</sup> This full-scale flight demonstration would be used to further the goal of the National Aeronautics and Space Administration (NASA) to mature compliant structure technologies that provide structural load alleviation, increase control surface effectiveness, improve aerodynamic efficiency and allow noise reduction. At the NASA Armstrong Flight Research Center (AFRC) (Edwards, California) there is a Gulfstream III (GIII) aircraft (Gulfstream Aerospace Corporation, Savannah, Georgia), tail number 804, which serves as a testbed for aeronautics flight research experiments. In late 2009, the AFRL and the NASA Environmentally Responsible Aviation (ERA) project partnered to integrate this GIII aircraft and flight-test the Adaptive Compliant Trailing Edge (ACTE) flap technology designed and built by FlexSys. This partnership of incorporating FlexSys proprietary technology as a full-scale flight demonstration of an adaptive compliant structure led to an extremely successful ACTE flight-testing campaign in 2015 on the NASA AFRC GIII Subsonic Research Aircraft Testbed (SCRAT) shown in Figure 1. The ACTE flaps were flight-tested at deflections ranging from -2° (up) to +30° (down) in order to validate the structural effectiveness and airworthiness of the

ACTE flaps. All partners contributed to different aspects of the ACTE program: the AFRL and the NASA ERA project were responsible for overall project management and execution; FlexSys was accountable for the compliant flap design and fabrication; and NASA AFRC was accountable for systems integration and flight-test execution. The NASA AFRC airworthiness process was followed to ensure all ACTE safety-of-flight aspects were met. This paper documents the details of the airworthiness process related to the aeroelastic effects of integrating the ACTE flaps onto the SCRAT.

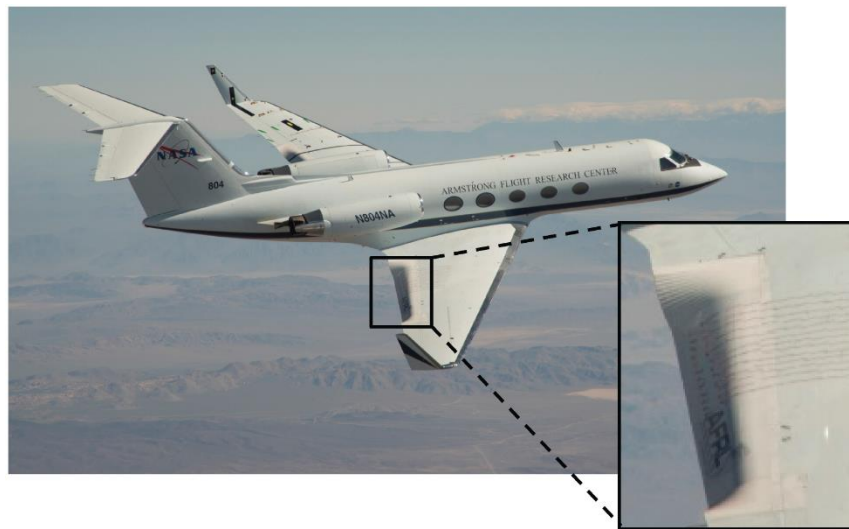


Figure 1. The ACTE flaps at 30° of deflection flown on SCRAT.

#### **4. THE NASA AFRC AIRWORTHINESS PROCESS**

The compliant, unconventional flaps required a multidisciplinary airworthiness assessment in order to integrate and safely flight-test the ACTE flaps on the SCRAT. The NASA AFRC airworthiness process entails numerous reviews throughout the life cycle of the project, evaluating the project design, testing, analysis, and flight-test plan to ensure all safety-of-flight requirements are being met. One of the ACTE multidisciplinary airworthiness assessments was to evaluate the aeroelastic effects of integrating the ACTE flight article to ensure the combined SCRAT and ACTE system was safe to fly within the desired flight envelope defined to achieve the required ACTE technical goals. The SCRAT and ACTE system needed to show a flutter-free flight envelope 20 percent greater than the ACTE flight envelope to satisfy the project requirements for demonstration of aeroelastic airworthiness. Several challenges were posed due to some of the non-linear characteristics of the deformation of the FlexSys test article; therefore, the aeroelastic assessment dictated extensive testing and analysis methods to support the demonstration of sufficient flutter margins. To minimize the impact to the ACTE flight schedule and attempt to accurately model the flight article, a build-up test and analysis approach was developed using prototype test articles. This structural building block test and analysis approach ensured an early understanding of the dynamic response of the FlexSys innovative compliant structure. A series of ground vibration tests (GVTs) were conducted to provide modal characteristics to develop, validate, and update finite element models (FEMs) used for the flutter analyses that bound all flight configurations. Smaller prototype test articles representative of the

ACTE flap were built prior to the flight articles and were used for this build-up ground testing and analysis approach. Numerous FEMs were developed using data from FlexSys and the ground tests. The FEMs were then incorporated into the SCRAT aircraft FEM to generate multiple combined SCRAT and ACTE FEMs that could be analyzed for aeroelastic instabilities. The aeroelastic analysis results showed the combined system of aircraft and flaps were predicted to have the required flutter margin to successfully demonstrate the adaptive compliant technology. Based on the analysis, accelerometers were installed throughout the ACTE flaps to capture the in-flight aeroelastic response. Flight-testing was conducted and flight data were acquired to validate the pre-flight analysis.

## 5. TEST ARTICLE OVERVIEW

The flight-test system consisted of the ACTE flaps integrated on the NASA SCRAT. An overview of both components is provided in the following sections.

### 5.1 Overview of the ACTE Flaps

The ACTE flight-test article consisted of two compliant flaps that replaced the NASA SCRAT conventional Fowler flaps on both the left and right sides of the aircraft. Figure 2 shows the ACTE flight-test article installed on the SCRAT. Each ACTE flap measures approximately 19 by 2 ft and entirely replaces the corresponding Fowler flap. The ACTE flaps attach to the aircraft at the same wing attachment points as the Fowler flaps. Each test article consisted of five main components: the inboard transition section (ITS); the main flap section; the outboard transition section (OTS); the flap spar; and the actuation system. The flap spar covered the span length of the flap, carried the attaching hardware, and held the actuation system. The actuation system was used to deflect the ACTE flaps through the operational range of deflection of  $-2^\circ$  (up) to  $+30^\circ$  (down), relative to the wing outer mold line (OML). The ACTE flaps were not actuated in flight, instead, they were configured on the ground before each flight.

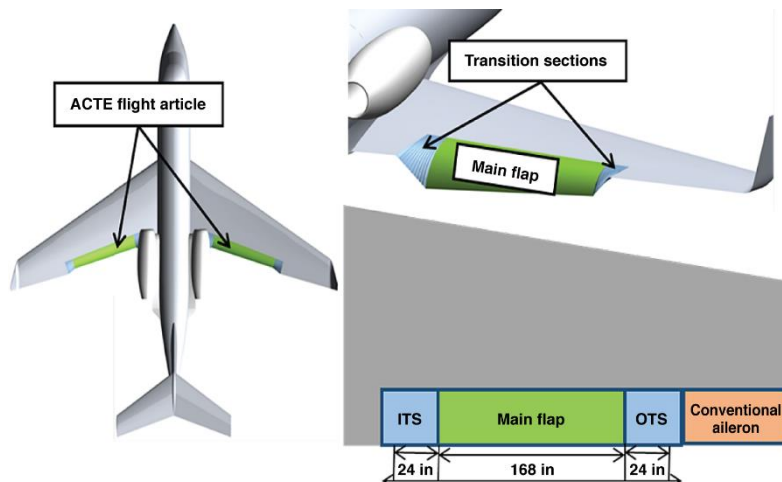


Figure 2. The ACTE flight-test article.

## **5.2 Overview of SCRAT**

The SCRAT is a GIII aircraft<sup>10</sup> modified by the NASA AFRC to support flight research experiments intended for advancing technologies. A transport-type air vehicle, the GIII facilitates aeronautics research related to transport flight regimes. An instrumentation system was installed to enable acquisition of research data, and a telemetry system transmits the data to the control room, where researchers and engineers monitor research experiments and safety-related information. The baseline SCRAT flight characteristics were established and evaluated in the summer of 2012. Baseline analytical models for all disciplines were further developed using these flight data to better understand the effects of future additions or modifications made to the SCRAT in support of flight projects such as ACTE.<sup>11</sup> Several modifications were performed to prepare the SCRAT to receive the ACTE installations. The Fowler flaps, ground and flight spoilers, and all associated hardware were removed from the SCRAT.

## **6. GROUND TESTING APPROACH**

Ground testing was an important part of the ACTE project approach toward showing an airworthiness assessment that incorporated conventional design practices. The approach followed a building-block testing and model validation approach. Numerous ground tests were conducted over the life cycle of the ACTE project to ensure the airworthiness of the structure. These ground tests consisted of material characterization testing, structural proof testing, structural qualification testing, fatigue testing, and ground vibration testing.

### **6.1 Build-up Approach**

The ACTE project incrementally worked up to the full-scale flight article flaps using a build-up testing approach; thus, the team could detect and correct any design and fabrication flaws early in the life cycle process to minimize major schedule delays and cost increase. This methodology also gave opportunity to gain early insight into the compliant structure technology. Finite element models were also validated along the way, building confidence in the modeling approach for these unconventional flaps. Prototype test articles representative of the ACTE flap design and fabrication process were built prior to the flight articles and were used for this build-up ground test approach. These prototypes provided learning opportunities to ensure the full-scale ACTE flaps would meet the necessary airworthiness requirements.

An illustration of the building-block testing approach with the planned structural dynamics tests required for the aeroelastic airworthiness assessment is highlighted in Figure 3. These structural dynamics tests included both material characterization and GVTs, which were necessary for the FEM development and validation. The planned testing in the build-up approach shown toward the top of the pyramid highlights a “Mated SCRAT + ACTE GVT” with the full-scale flight test article; however, this test was eventually deemed unnecessary to further refine the FEM.

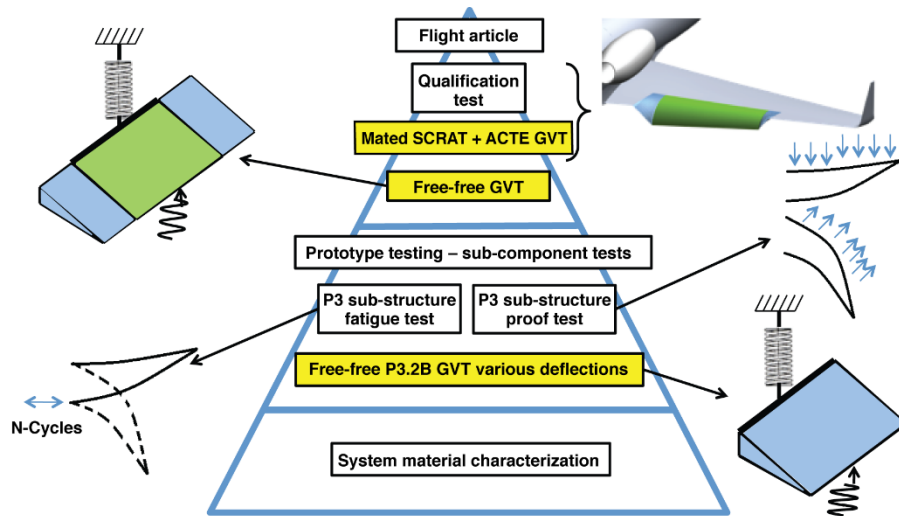


Figure 3. The ACTE building block testing approach.

## 6.2 Prototype Ground Vibration Testing

Several prototypes were fabricated for developmental efforts. A GVT was conducted on the prototype, denoted as prototype 3.2B (P3.2B), which was a full-scale, right-side ITS with an extension of the flap spar. The P3.2B GVT data were used to develop correlation methods for the ACTE FEMs. This test helped to gain confidence in testing and understanding the ACTE modal characteristics needed for the FEM development and validation. This prototype GVT was executed by NASA personnel at the FlexSys facility in April 2013. The test objectives were to measure the test article frequencies and mode shapes with deflections of  $-2^\circ$ ,  $0^\circ$ , and  $+30^\circ$ . Figure 4 shows P3.2B GVT setups. The P3.2B GVT was conducted with a free-free boundary condition. The purpose of these GVTs was to quantify the change in frequencies and mode shapes as a function of flap deflection, evaluate accelerometers as instrumentation on the flexible structure, and evaluate various types of excitation methods and analytical FEM techniques employed.

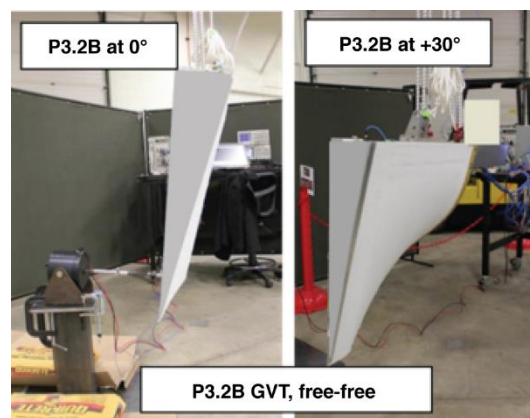


Figure 4. Prototype 3.2B ground vibration test setups.

This prototype GVT provided a comprehensive set of lessons learned regarding modeling the ACTE flap, testing unconventional structures such as the ACTE flap, and updating the FEM. One of the most useful insights from the prototype testing was the variation of the flap modes and frequencies as a function of deflection. An unexpected outcome of this GVT was the high damping values due to characteristics of the flexible structure. The frequencies of all five mode shapes decreased with higher deflections from  $-2^\circ$  to  $+30^\circ$ . As anticipated, the difference between  $-2^\circ$  and  $0^\circ$  was barely noticeable, with the most change occurring in their second mode, overall mode 3, with a difference of 1.2 Hz. The greatest change observed was in mode 6, with a difference of 5.3 Hz from  $-2^\circ$  to  $+30^\circ$ . Table 1 shows how the analytical results compared with the P3.2B GVT results. Overall, the analytical frequencies are lower than those for the test results for the modes of interest. The P3.2B GVT  $+30^\circ$  configuration revealed an unpredicted mode, shown as overall mode 2 in Table 1 and in Figure 5, and possibly caused by lower stiffness as a result of the truncated P3.2B span-wise main flap section.

Table 1. Prototype 3.2B GVT versus analytical FEM frequency comparison.

GVT vs. Analytical FEM									
Mode	Frequency, Hz								
	$-2^\circ$ Up			$0^\circ$			$+30^\circ$ Down		
	Test (Hz)	FEM (Hz)	% Change	Test (Hz)	FEM (Hz)	% Change	Test (Hz)	FEM (Hz)	% Change
1	31.42	27.21	-13%	31.07	26.78	-14%	28.45	29.61	4%
2	---	---	---	---	---	---	29.51	---	---
3	38.22	33.51	-12%	37.0	33.08	-11%	35.49	31.70	-11%
4	42.28	39.33	-7%	42.05	38.75	-8%	37.66	37.37	-1%
5	46.38	45.07	-3%	46.22	44.48	-4%	42.29	44.52	5%
6	50.36	46.45	-8%	50.36	46.62	-7%	44.99	45.34	1%

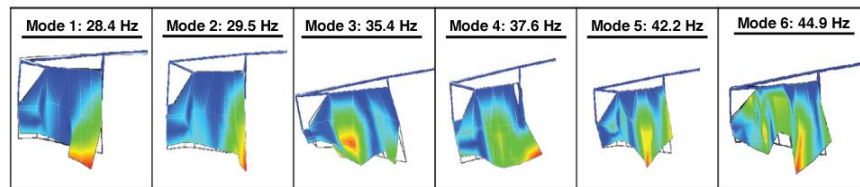


Figure 5. Prototype 3.2B ground vibration test mode shapes for the flap at  $30^\circ$  of deflection.

### 6.3 Flight Article Right Flap Free-Free Ground Vibration Testing

The ACTE flight article right side flap free-free GVT was the third modal test conducted by NASA personnel and was performed at the NASA AFRC Flight Loads Laboratory (FLL) in March 2014. The ITS was the same design as what was previously tested for P3.2B. The test objectives were to measure the ACTE right flap structural frequencies, mode shapes, and damping data at the three flap deflections of  $0^\circ$ ,  $+15^\circ$  and  $+30^\circ$  with a free-free boundary condition so that the FEM could be validated and updated. Prior to performing the flight article free-free GVT, a weight and center of gravity measurement of the flap was carried out.



Figure 6 shows the GVT setup with the ACTE right flap in a free-free boundary condition. This boundary condition utilized an overhead soft suspension system made from two custom bungees connected from the test article to the upper fixture and then with a load cell going to the overhead crane hook in the FLL. Excitation was provided by using a shaker supported on a shaker stand and attached to the test article using a conventional stinger at five locations for the 0° configuration and at two of the five locations for the 15° and 30° flap configurations.

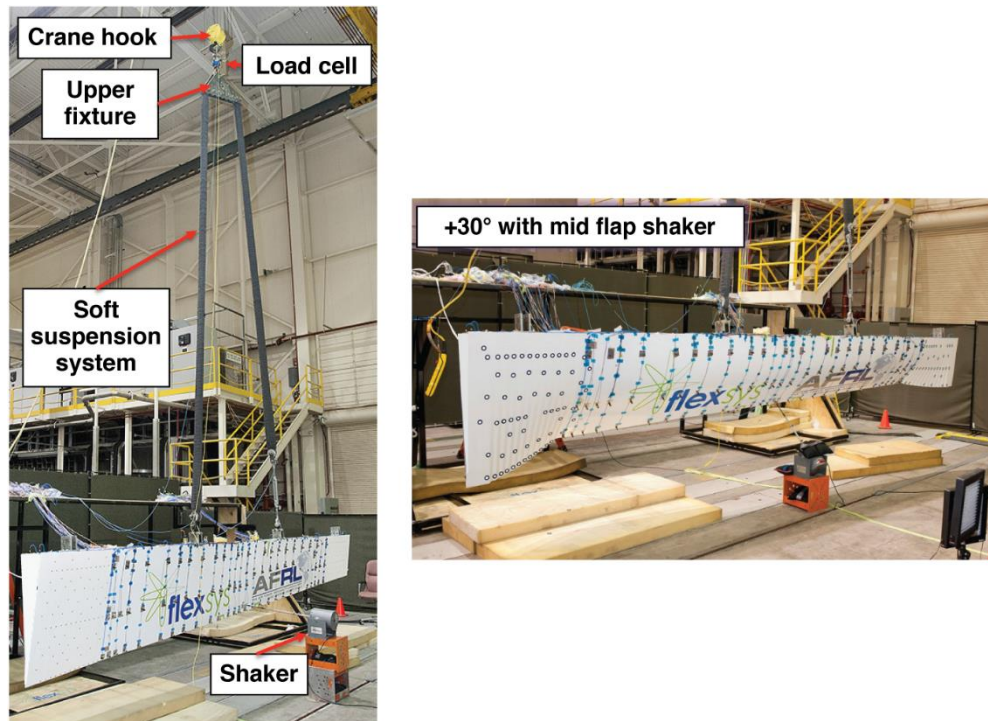


Figure 6. The ACTE right flap free-free ground vibration test setup.

The results from the right flap free-free GVT at different flap deflections are shown in Figure 7. Only the right flap was tested; symmetry from left to right was assumed. After these GVT data were analyzed, the flap FEM was updated and mated to the SCRAT FEM. A flutter analysis was performed using this combined FEM, and updated flutter margins were generated. The flutter margins beyond the ACTE flight envelope were very high (~75 percent), so a “Mated SCRAT + ACTE GVT” (the fourth GVT planned in the build-up testing approach) was deemed unnecessary to further refine the FEM.



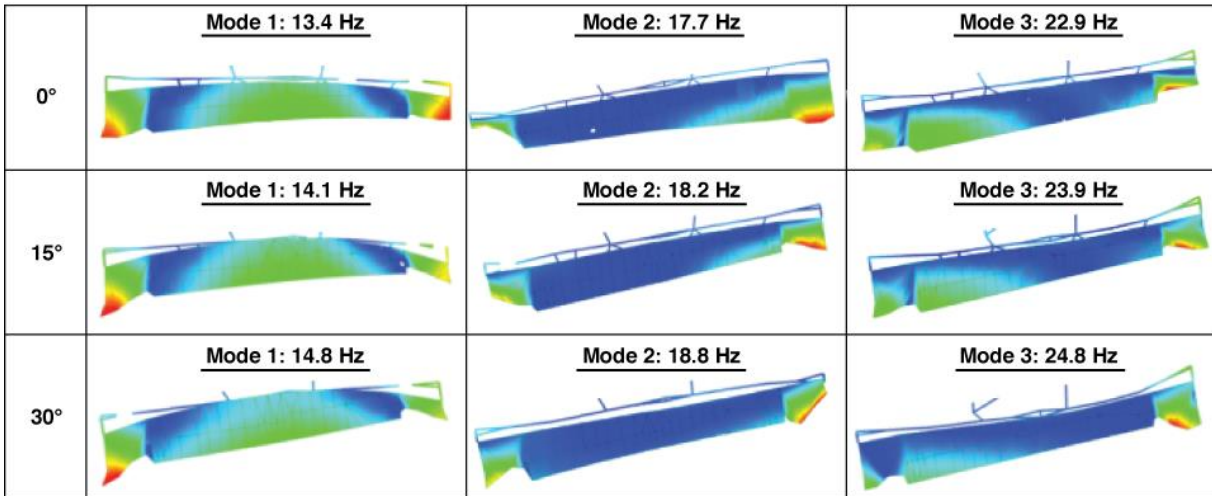


Figure 7. Ground vibration test results for the ACTE right flap at different deflections.

## 7. AEROELASTIC ANALYSIS

When the Fowler flaps of the SCRAT aircraft were replaced by the ACTE flaps, the aircraft as well as the new flaps needed to be cleared for flutter within the ACTE flight envelope. Flutter is a subset of aeroelasticity which involves the interactive superposition of aerodynamic, elastic, and inertial forces on structures to produce an unstable oscillation that often results in structural failure. Representative aeroelastic analyses that are performed are required to predict that the modified aircraft is free of flutter within the flight envelope plus a 20-percent margin. The flutter clearance procedure involves the combination of pre-flight flutter analysis and flight flutter testing. The pre-flight flutter analysis for the SCRAT aircraft with the ACTE flaps installed requires a structural FEM which was updated based on the GVT results and an aerodynamics model based on a linear panel method. The baseline aircraft FEM was updated using GVT data from a previous project.

### 7.1 Model Correlation

A FEM was created for the ACTE flap using a typical combination of shell and beam elements. The model was built by FlexSys using ANSYS® (Canonsburg, Pennsylvania)<sup>12</sup> eight-node quadrilateral element for stress calculation, converted to four-node quadrilateral element in MSC Nastran™ (Newport Beach, California)<sup>13</sup> format for modal analysis. The flap FEM contains 44,060 nodes and 66,300 elements and is shown in Figure 8. The ACTE flap contains an ITS and an OTS, and a main flap section. During the modeling of the ACTE flap, the biggest challenge was the modeling of the transition sections due to the large deflections of the flexible structure. The modal analysis is linear, so the material properties for the transition sections had to be linearized. In order to obtain the equivalent linear material properties for the transition sections, a build-up approach tuning the FEM with GVT data was used. During the ACTE manufacturing stages, the ITS was built first, allowing an FEM of the ITS to be developed and correlated to prototype GVT data in advance of performing the flight article GVT. The final full-flap FEM was then correlated with the full-flap GVT results with high confidence.

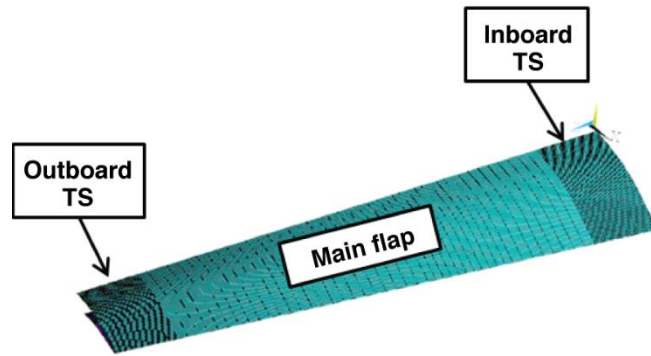


Figure 8. The finite element model of the ACTE flap.

## 7.2 Prototype Model Correlation

The P3.2B FEM extracted from the full ACTE flap model for model correlation is shown in Figure 9. This prototype model contains 14,210 nodes and 22,724 elements. Figure 10 presents the vibration mode shapes from a modal analysis using MSC Nastran™. The analysis predicted a general decrease in the frequencies as a function of deflection with the exception of mode 5. Mode 1 showed the greatest decrease of 3.2 Hz. Mode 5 showed an increase of 1.7 Hz. The trend in decreasing frequency generally matched what was observed in the P3.2B GVT.

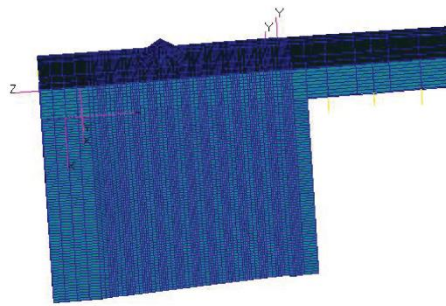


Figure 9. The finite element model of the P3.2B.

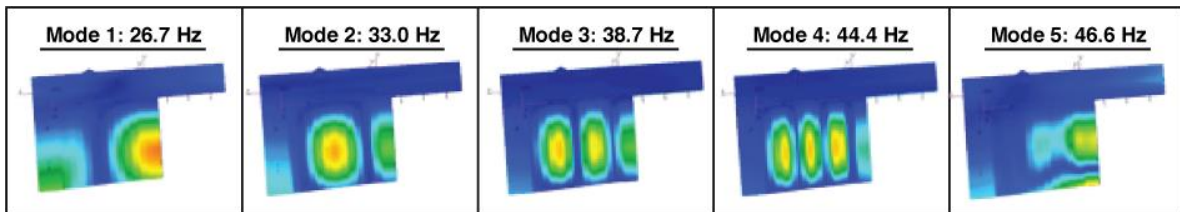


Figure 10. The first five elastic modes from the 0-deg flap configuration for the prototype 3.2B FEM.

### 7.3 Flight Article Model Update

After the validation of the prototype model was completed, the material properties used in the prototype were inserted into the full-flap FEM. The final full-flap FEM was validated and updated using the full-flap GVT results. The full-flap flight article was tested at configurations  $0^\circ$ ,  $15^\circ$ , and  $30^\circ$  in order to obtain the trend of the frequency change for the different flap angles. The frequencies showed an increase as a function of deflection, which was the opposite of what occurred with the P3.2B. The addition of the main flap and the increase in internal strain as a function of deflection created an apparent augmentation in stiffness. Figure 11 shows the vibration mode shapes for the  $0^\circ$  configuration. Natural frequencies for configurations of  $0^\circ$ ,  $15^\circ$ , and  $30^\circ$  are summarized in Table 2.

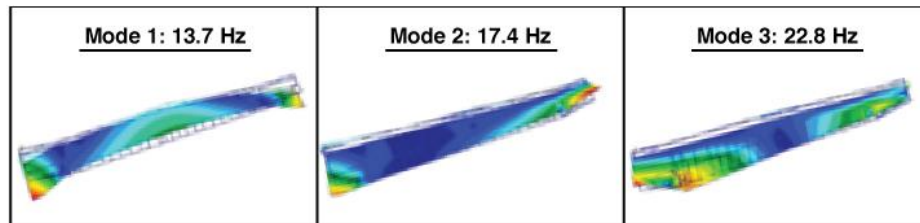


Figure 11. The first three full-flap finite element model elastic modes from the  $15^\circ$  configuration.

Table 2. Natural frequencies for different full-flap configurations.

Mode	Frequency, Hz		
	$0^\circ$ (Wing OML)	$15^\circ$ (Down)	$30^\circ$ (Down)
1	13.7	14.1	14.9
2	17.4	18.5	19.2
3	22.8	23.8	23.8

### 7.4 Analysis versus Test

By comparing analysis results with the GVT results, the final flap FEM shows good correlation. Frequency comparison between FEM results and the GVT data for the configurations of  $0^\circ$ ,  $15^\circ$ , and  $30^\circ$  are summarized in Table 3. The frequency matching requirement was 5.0 percent based on a NASA standard for modeling.<sup>14</sup> The first three modes were chosen as required correlated modes based on the frequency range used in the flutter analysis. Mode 3 had the highest frequency correlation error for the  $30^\circ$  deflection of 4.6.

Table 3: Full-flap frequency comparison of FEM and GVT for  $0^\circ$ ,  $15^\circ$ , and  $30^\circ$  configurations.

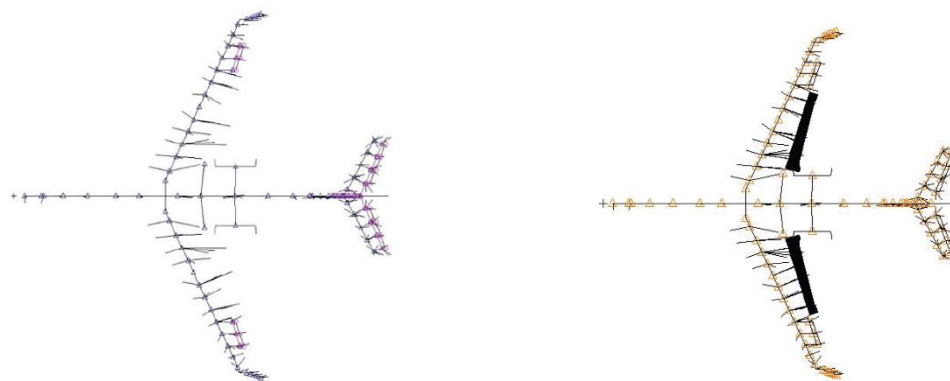
Mode	$0^\circ$ (Wing OML)			$15^\circ$ (Down)			$30^\circ$ (Down)		
	FEM (Hz)	GVT (Hz)	Delta	FEM (Hz)	GVT (Hz)	Delta	FEM (Hz)	GVT (Hz)	Delta
1	13.7	13.4	-2.2%	14.1	14.1	0.0%	14.9	14.8	-0.7%
2	16.8	17.4	3.6%	18.5	18.3	-1.1%	19.2	18.8	-2.1%
3	23.1	22.8	-1.3%	23.8	23.9	0.4%	23.8	24.9	4.6%

## 7.5 Pre-flight Analytical Predictions

The pre-flight flutter analysis was used to identify the flutter characteristics of the combined system and establish broad trends over the flight envelope and provide the guideline for planning the flutter flight test. Flutter computations involve structural modal analysis from which the frequencies and mode shapes are incorporated into aerodynamic model for flutter analysis. The results of these computations are used in the control room to fully assess the airworthiness of the flight system.

## 7.6 Structural Model Analysis

The baseline SCRAT FEM model was developed by NASA AFRC and ATA Engineering, Inc. (San Diego, California) personnel using a half-GIII aircraft FEM obtained from Gulfstream and modified to represent the NASA SCRAT. The FEM model is a stick model containing only beam elements. The structural modal analysis was performed using a FEM which was updated based on the results obtained by performing a baseline GVT on the GIII structure. The original Fowler flaps, modeled as point masses, were removed from the baseline aircraft FEM. The ACTE flap models were then added to the stick model using MSC Nastran™ CBUSH elements. Figure 12 shows the FEM for the baseline SCRAT aircraft and the combined ACTE flaps. Typical lower elastic mode shapes from the modal analysis are shown in Figure 13.



(a) Baseline SCRAT finite element model. (b) SCRAT with ACTE flaps.

Figure 12. The SCRAT finite element model with and without ACTE flaps.

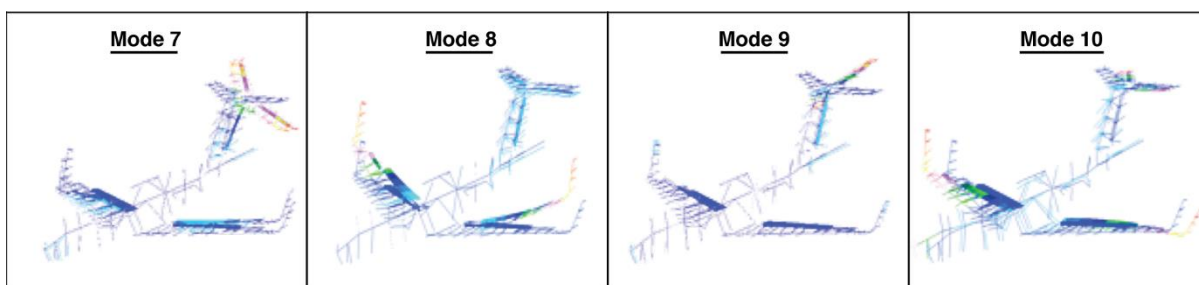


Figure 13. Lower elastic mode shapes for the SCRAT aircraft with ACTE flaps FEM.

## 7.7 Flutter Analysis

Aircraft flutter involves divergent structural oscillations with the potential to result in catastrophic destruction. Flutter analyses were performed using ZAERO™ (Scottsdale, Arizona)<sup>15</sup> matched point procedure by fixing the altitude and changing the speed or by fixing the speed and changing the altitude for the analyses. The AFRC project team developed the baseline SCRAT aerodynamic model from a half-aerodynamic model and updated it to a full SCRAT aerodynamic model that included the ACTE flaps and contains 3021 flat panel elements as shown in Figure 14. Flutter analyses were carried out for two typical fuel conditions: full fuel and empty fuel, with flap configurations of 0°, 30°, and -2° flap configurations. The calculated flutter speeds for higher Mach numbers across the range of flap deflections are summarized in Tables 4 and 5. Typical flutter results which include velocity versus frequency (v-f) plot and velocity versus damping (v-g) plot for Mach number 0.8 are shown in Figure 15. The predicted flutter occurs when the damping trace rises above the assumed 2-percent structural damping. The damping signs are positive since the convention is for the damping value required to suppress flutter.

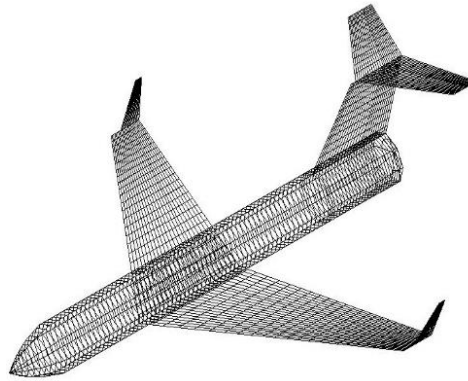


Figure 14. The SCRAT aerodynamic model.

Table 4. Flutter prediction boundary for different flap angles (empty fuel).

Flap Angle	Mach = 0.6			Mach = 0.7			Mach = 0.8		
	Speed (KEAS)	Frequency (Hz)	Altitude (ft)	Speed (KEAS)	Frequency (Hz)	Altitude (ft)	Speed (KEAS)	Frequency (Hz)	Altitude (ft)
<b>30</b>	739	10.3	-38000	690	3.4	-24000	640	3.4	-11200
<b>0</b>	680	10.9	-33200	660	3.4	-21900	615	3.4	-8430
<b>-2</b>	680	9.5	-33400	650	8.7	-20000	640	2.9	-11500

Table 5. Flutter prediction boundary for different flap angles (full fuel).

Flap Angle	Mach = 0.6			Mach = 0.7			Mach = 0.8		
	Speed (KEAS)	Frequency (Hz)	Altitude (ft)	Speed (KEAS)	Frequency (Hz)	Altitude (ft)	Speed (KEAS)	Frequency (Hz)	Altitude (ft)
<b>30</b>	-	-	-	800	3.4	-24000	740	5.7	-23200
<b>0</b>	700	3.4	-35000	640	3.3	-19200	580	3.3	-5470
<b>-2</b>	-	-	-	735	7.4	-27700	690	7.2	-15500

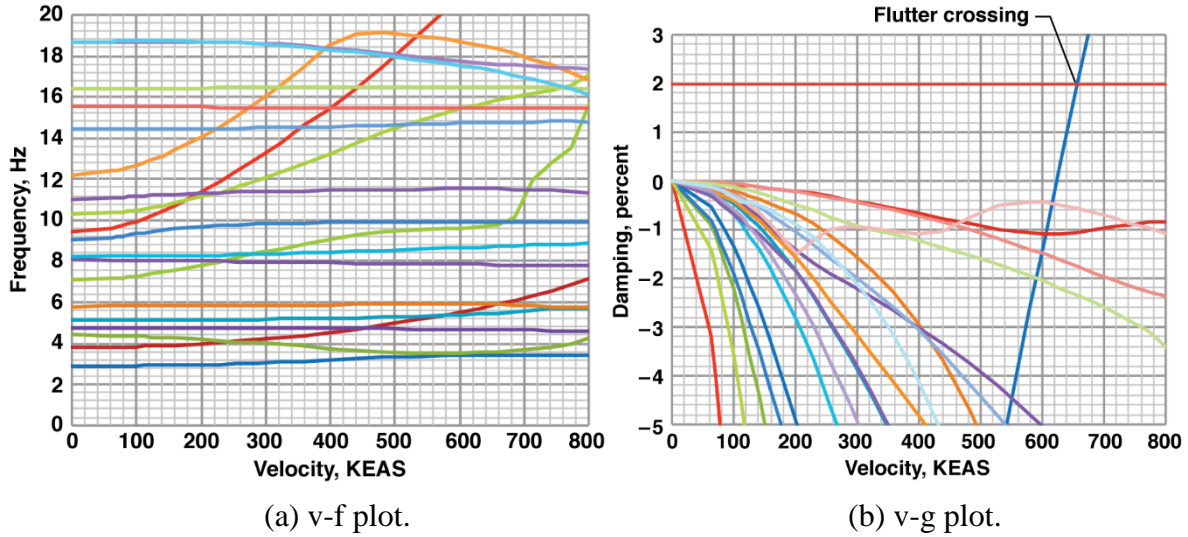


Figure 15. Typical v-f and v-g plots.

## 8. FLIGHT-TESTING APPROACH

Flight-testing of the ACTE flaps was performed from November of 2014 to April of 2015.<sup>16</sup> The ACTE flaps were deflected through their full operational range.

### 8.1 Pre-flight Analytical Predictions

As described above, a flutter analysis that was performed using a validated FEM produced the pre-flight analytical predictions that were used to validate the aeroelastic model of the flight system. A set of analytical predictions was developed for both empty fuel and full fuel SCRAT configurations and for ACTE deflections of  $0^\circ$ ,  $15^\circ$ , and  $30^\circ$ . These SCRAT and ACTE analytical frequency values were considered the flight-test anchor points in the validation of the aeroelastic models. The deflections that were not modeled were considered spot check points and were used to verify trends as opposed to validate models. Table 7 shows the list of modes tracked for the SCRAT and ACTE system during flight-testing with the ACTE deflection of  $0^\circ$ . Similar tables were generated for deflections of  $15^\circ$  and  $30^\circ$ . Table 6 includes modes that participate in the critical flutter mechanisms as well as ACTE modes that were tracked as a function of deflection.

Table 6. Pre-flight analytical predictions for SCRAT with the ACTE configured at  $0^\circ$ .

SCRAT with ACTE 0° (EMPTY FUEL)		SCRAT with ACTE 0° (FULL FUEL)	
Description	Freq.	Description	Freq.
Vertical Tail Bending	2.87	Vertical Tail Bending	2.61
Wing 1B Symm	3.43	Wing 1B symm	2.54
Wing 2B antisymm	7.87	Wing 2B antisymm	6.34
Fin torsion, Stab 1B antisymm	8.10	Fin torsion, Stab 1B antisymm	7.42
Wing 2B symm, elevator rot symm	8.46	Wing 2B symm	7.04
Wing 3B antisymm, ACTE OTS anti	12.99	Wing 3B antisymm, ACTE ITS anti	12.23
Wing 1T symm, ACTE ITS symm	14.89	Wing 1T symm, ACTE symm/stab symm	11.62
Wing 1T antisymm, ACTE ITS symm	15.43		
		Wing 3B symm, ACTE span bending	13.55
		Wing 3B antisymm, ACTE span bending	14.71
Winglet 1B symm, ACTE ITS symm	15.30	Winglet1B symm, ACTE ITS symm	18.44
Winglet 1B anti, ACTE span bend anti	16.04	Winglet 1B anti, ACTE ITS anti	16.45
Winglet 1B symm, ACTE span bend sym	16.97	Winglet 1B symm, ACTE span bending	15.27
Wing 1T anti, ACTE span bend anti	17.61		
		ACTE ITS symm	17.03
		ACTE OTS symm	17.27
Winglet 1B symm, ACTE ITS symm	19.28	Winglet symm, ACTE OTS	20.05
Winglet 1B anti, ACTE ITS anti	19.34	Winglet antisymm, ACTE OTS	20.23
Winglet 1B anti, ACTE ITS anti, engine pitch	19.91		
Wing 2T anti, ACTE flap rotation anti	21.77	Wing 2T anti, ACTE flap rotation anti	19.09
ACTE rotation anti	23.16		

## 8.2 Project Approach

Similar to the ground testing approach, the ACTE project used a build-up approach for the execution of flight-testing. The build-up approach entailed clearing the ACTE flight envelope starting from low altitude and slow speed, followed by high altitude and slow speed, thirdly by high altitude and fast speed to, finally, low altitude and fast speed. This strategically increases Mach number and dynamic pressure, and consequently, the risk of aeroelastic instability until the point of maximum Mach and maximum dynamic pressure is reached. The Mission Control Center (MCC) at AFRC was staffed to monitor key flight-testing parameters to ensure a safe and successful mission. A set of flight-test maneuvers was executed to acquire data that validated stability and controls models, structural analyses, and aeroelastic predictions at incremental speeds and flap settings. Figure 16 shows the ACTE flight envelope designed to demonstrate the structural effectiveness and further mature the compliant technology of the ACTE flaps.



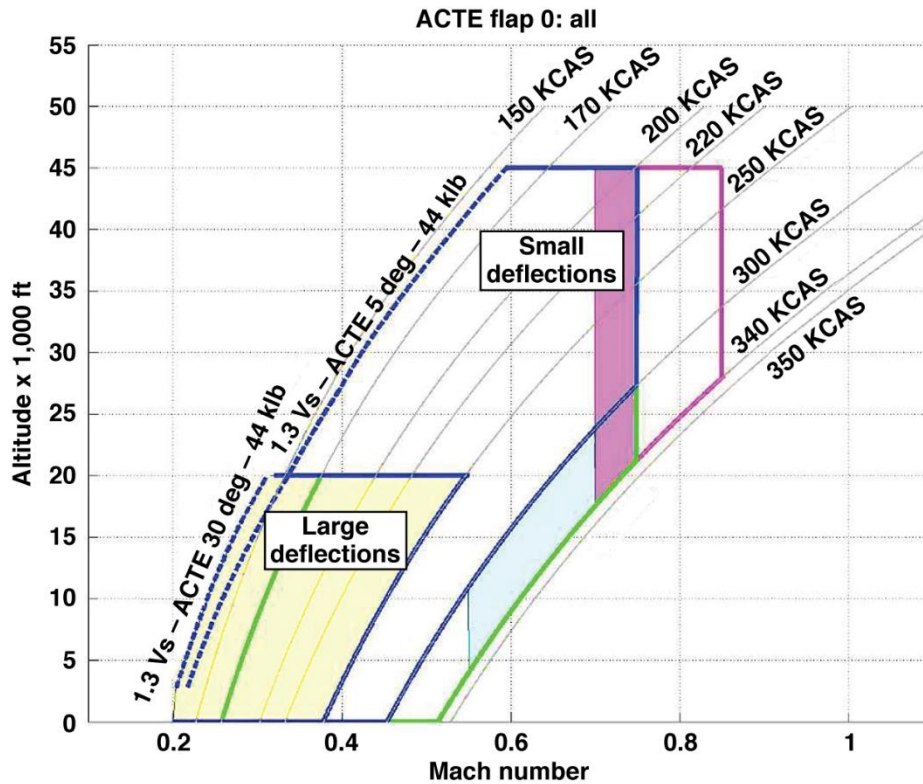


Figure 16. The ACTE flight envelope.

### 8.3 Flight-Test Instrumentation

The SCRAT aircraft was instrumented for baseline flight-testing. Additional instrumentation was installed on the ACTE as part of the airworthiness process. Each ACTE flap was instrumented for flight with 12 vertical accelerometers used to capture frequencies and mode shapes in flight. The accelerometer locations were chosen based on the results of the modal analysis. The instrumentation locations for the right ACTE flap are shown in Figure 17. High-rate strain gages that are not shown were used for additional backup sensors. The left-side ACTE flap instrumentation suite is a mirror of that on the right side of the SCRAT. All accelerometers were monitored by way of a telemetered data stream in the MCC at NASA AFRC.

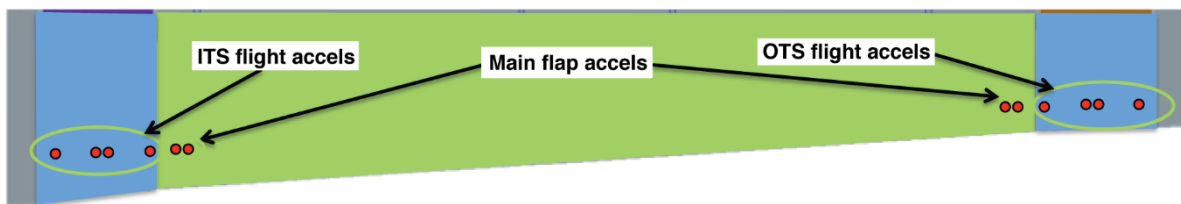


Figure 17. Right-side ACTE flap instrumentation.

### 8.4 Control Room Operations

The data were monitored from the MCC for the entire duration of each flight. At the NASA AFRC, Interactive Display System (IADS) software is used to display the data and perform

pseudo-real time analyses. Figure 18 shows an example of the displays used by Structural Dynamics engineers for monitoring aeroelastic responses. Time histories were monitored using the IADS strip charts, and power spectral density plots were calculated to evaluate frequency and damping. The half-power damping estimation provided in-flight measured damping values.

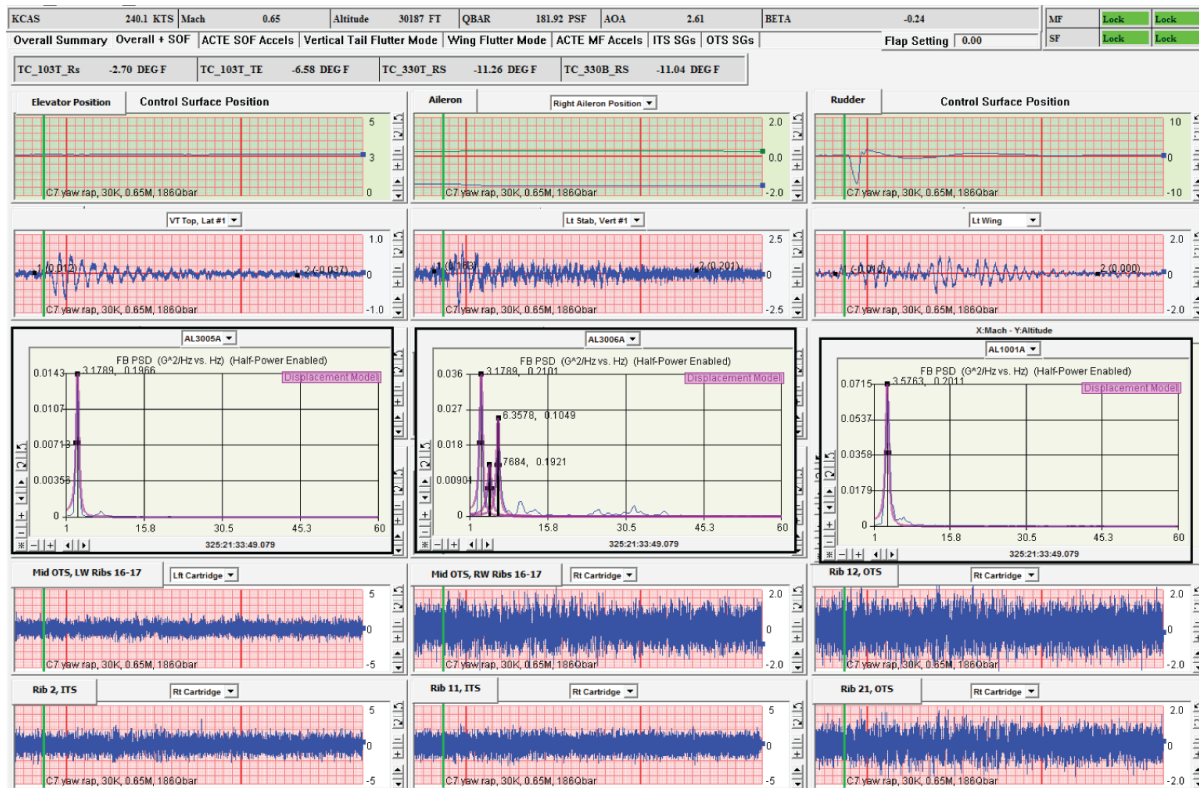


Figure 18. An example of the Structural Dynamics control room display.

## 8.5 SCRAT and ACTE In-flight Aeroelastic Response

The SCRAT possesses no flutter excitation system, therefore, control surface raps were used to input an impulsive force into the structure to excite the resonant modes. Pitch, roll, yaw raps, and various other aircraft maneuvers that produced higher frequency turbulence were utilized to ensure all modes of interest were excited. The results showing the frequency and damping for the modes of greater significance of the ACTE at  $0^\circ$  are listed in Table 7. The results reported were measured at a maximum Mach number and dynamic pressure flight condition.

Table 7. In-flight aeroelastic response of the ACTE configured at 0° deflection.

<b>Mode Description</b>	<b>Freq. (Hz)</b>	<b>Damping (%)</b>
Vertical tail bending	3.18	16.6
Stab 1B anti	4.37	25.8
Wing 2B antisymm	7.15	13.4
Wing 3B anti, Left ACTE OTS anti	11.19	7.6
Wing 3B anti, Right ACTE OTS anti	12.21	12.1
Wing 3B symm, ACTE span bending	13.22	11.2
Wing 1T antisymm, ACTE ITS symm	15.77	7.3
Winglet 1B symm, ACTE span bend symm	16.28	13.9
Wing 1T anti, ACTE span bend anti	17.80	8.8
Winglet 1B symm, ACTE ITS symm	18.82	4.2
Winglet 1B anti, ACTE ITS anti	19.33	9.8

The flight-test results are correlated to validate and give confidence in the analytical values. The ACTE flight article showed some asymmetries that were not in the baseline aircraft as reported in Table 7 above. Table 8 shows the comparison with both empty and full fuel SCRAT and ACTE models since flight-test data were acquired between those fuel conditions. The flight-test frequencies outside of the empty to full fuel FEM bounds can be attributed to the aerodynamic effects on modal frequency that are not included in the FEM results. For example, the vertical tail bending mode frequency was predicted to increase slightly with velocity, as shown in the velocity-frequency plot in Figure 15 (a) as the lowest frequency mode in blue.

Table 8. Comparison of flight-test results with analytical values for the ACTE configured at 0° deflection.

<b>Mode Description</b>	<b>FEM Empty Fuel (Hz)</b>	<b>Flight Test (Hz)</b>	<b>FEM Full Fuel (Hz)</b>
Vertical tail bending	2.87	3.18	2.61
Stab 1B anti	4.40	4.37	4.31
Wing 2B antisymm	7.87	7.15	6.34
Wing 3B anti, Left ACTE OTS anti	12.99	11.19	10.90
Wing 3B anti, Right ACTE OTS anti	12.99	12.21	10.90
Wing 3B symm, ACTE span bending	--	13.22	13.55
Wing 1T antisymm, ACTE ITS symm	15.43	15.77	--
Winglet 1B symm, ACTE span bend symm	16.97	16.28	15.27
Wing 1T anti, ACTE span bend anti	17.61	17.80	--
Winglet 1B symm, ACTE ITS symm	19.28	18.82	--
Winglet 1b anti, ACTE ITS anti	19.34	19.33	16.45

## 8. SUMMARY AND CONCLUSIONS

The National Aeronautics and Space Administration (NASA) Armstrong Flight Research Center (AFRC) partnered with several organizations to demonstrate the structural effectiveness of two unconventional lifting surfaces that enable a continuous mold line on transport aircraft. The Adaptive Compliant Trailing Edge (ACTE) flaps were integrated onto the NASA Subsonic Research Aircraft Testbed (SCRAT) aircraft to accomplish this goal. Due to a variety of unique characteristics of the ACTE structure and to lower the risk to mission success, a build-up approach was employed in how to model and test the structure. A series of ground vibration tests were performed on prototypes to establish the experience needed to model the flight-test article accurately. Using these data, an accurate, combined model of the SCRAT and ACTE flight system was developed and pre-flight analytical predictions were produced. These pre-flight predictions showed compliance with the requirement for a flutter margin of at least 20 percent for all flight-test configurations. The analytical predictions contributed to lowering risk in the flight clearance process. Control surface raps were used to excite the SCRAT and ACTE system and measure frequencies for the modes of interest to compare with the analytical predictions and verify sufficient flutter margin existed. The aeroelastic airworthiness assessment of the ACTE flight-test article was completed and the flight-test results compared well with the pre-flight analytical predictions. The build-up approach employed to clear the ACTE flaps proved to be effective and sufficient.

## 9. REFERENCES

1. Kota, S., Hetrick, J., Osborn, R., Paul, D., Pendleton, E., Flick, P., and Tilmann, C., "Design and Application of Compliant Mechanisms for Morphing Aircraft Structures," *Proc. of SPIE*, Vol. 5054, 2003, pp. 24-33.
2. Kota, S. "Compliant Systems using Monolithic Mechanisms," *Smart Materials Bulletin*, Volume 2001, Issue 3, pp. 7-10.
3. Kota, S., Hetrick, J. A., and Osborn, R. F. Jr., "Adaptive Structures: Moving into the Mainstream," *Aerospace America*, September 2006, pp. 16-18.
4. Kota, S., Osborn, R., Ervin, G., Maric, D., Flick, P., and Paul, D., "Mission Adaptive Compliant Wing – Design, Fabrication and Flight Test," paper RTO-MP-AVT-168.
5. Kota, S., Ervin, G., Osborn, R., and Ormiston, R., "Design and Fabrication of an Adaptive Leading Edge Rotor Blade," American Helicopter Society 64th Annual Forum, Montreal, April 29-May 1, 2008.
6. Gilyard, G., and Espana, M., *On the Use of Controls for Subsonic Transport Performance Improvement: Overview and Future Directions*, NASA TM 4605, August 1994.
7. Tilmann C., Flick P. M., Martin C. A., and Love, M. H., "High-Altitude Long Endurance Technologies for SensorCraft," paper RTO-MP-104.

8. Reed, S. A., "High Altitude Long Endurance Airfoil Performance Validation," WL-TR-96-3091, January 1996. Available from WL/FIMA, Wright-Patterson AFB, Ohio, 45433-7913.
9. Greff, E., "The Development and Design Integration of a Variable Camber Wing for Long/Medium Range Aircraft," *Aeronautical Journal*, Vol. 94, No. 939, November 1990, pp. 301-312.
10. Department of Transportation, Federal Aviation Administration, "Type Certificate Data Sheet No. A12EA," Revision 44, May 11, 2015.  
[http://rgl.faa.gov/Regulatory\\_and\\_Guidance\\_Library/rgMakeModel.nsf/0/9822d5951d15263986257e4500581a16/\\$FILE/A12EA\\_Rev\\_44.pdf](http://rgl.faa.gov/Regulatory_and_Guidance_Library/rgMakeModel.nsf/0/9822d5951d15263986257e4500581a16/$FILE/A12EA_Rev_44.pdf). Accessed August 31, 2015.
11. Baumann, E., Hernandez, J., and Ruhf, J., "An Overview of NASA's Subsonic Research Aircraft Testbed (SCRAT)," AIAA-2013-5083, August 2013.
12. *ANSYS Mechanical User's Guide*, ANSYS Inc., Canonsburg, Pennsylvania, Release 15.0, November 2013.
13. *MSC Nastran 2010 Quick Reference Guide*, MSC Software Corporation, Santa Ana, California, 2010.
14. National Aeronautics and Space Administration, "Load Analyses of Spacecraft and Payloads," NASA-STD-5002, June 21, 1996.
15. *ZAERO User's Manual Version 8.2*, ZONA Technology Inc., Scottsdale, Arizona, 2008
16. <http://www.nasa.gov/press-release/nasa-successfully-tests-shape-changing-wing-for-next-generation-aviation>. Accessed August 31, 2015.

## **10. BIOGRAPHY**

Claudia Herrera holds a Bachelor of Science Degree in Mechanical Engineering from the University of Texas at El Paso. She has been with NASA Armstrong Flight Research Center since January of 2005, and works there as a Structural Dynamics engineer. Claudia is involved in the life cycle phase of flight-test projects that take finite element models to flight-test validation, participating in both the analytical and test aspects of model correlation and verification. She performs modal and flutter analyses on various types of airframes as well as on external stores and flight experiments that use NASA flight-test platforms. Claudia also performs ground vibration tests to acquire and provide data to validate or update the analytical models used to create pre-flight predictions. She then supports the flight-testing effort, where the culmination of both the analytical and test work occurs and models are verified.